Radiology

Cardiac MR Strain: A Noninvasive Biomarker of Fibrofatty Remodeling of the Left Atrial Myocardium[1]

Adrian T. Huber, MD, MSc
Jérôme Lamy, MSc
Amer Rahhal, MD
Morgane Evin, PhD
Fabrice Atassi, PhD
Carine Defrance, MD
Guillaume Lebreton, MD
Karine Clément, MD, PhD
Myriam Berthet, MSc
Richard Isnard, MD, PhD
Pascal Leprince, MD, PhD
Philippe Cluzel, MD, PhD
Stéphane N. Hatem, MD, PhD
Nadjia Kachenoura, PhD
Alban Redheuil, MD, PhD

Purpose: To determine whether left atrial (LA) strain quantification with cardiac magnetic resonance (MR) imaging feature tracking is associated with the severity of LA fibrofatty myocardial remodeling at histologic analysis.

Materials and Methods: This prospective case-control study was approved by the institutional review board. LA strain was evaluated with cardiac MR feature tracking between January 2014 and March 2015 in 13 consecutive patients (mean age, 61 years ± 19; nine male) with mitral regurgitation in the 24 hours before mitral valve surgery and 13 age- and sex-matched healthy control subjects. LA strain parameters were compared first between control subjects and patients and then according to atrial fibrillation and mitral regurgitation status. Associations between LA strain and histology of preoperative biopsies were reported by using receiver operating characteristic curve analysis and Spearman correlation.

Results: Peak longitudinal atrial strain (PLAS) was significantly lower in patients with mitral regurgitation than in healthy control subjects ($P < .001$). Increased LA remodeling was significantly related to altered LA strain, and the strongest association was found between PLAS and the degree of fibrofatty myocardial replacement at histologic analysis ($r = -0.75$, $P = .017$). LA end-diastolic volume was increased in patients with mitral regurgitation when compared with that in healthy volunteers ($P < .001$) because of volume overload; however, volume did not correlate with the histologic degree of LA fibrofatty replacement ($r = -0.35$, $P = .330$).

Conclusion: LA strain, especially PLAS, correlates strongly with the degree of fibrofatty replacement at histologic analysis. Such functional imaging biomarker in combination with LA volumetry could help to guide clinical decisions, since myocardial structural remodeling is a known morphologic substrate of LA dysfunction leading to atrial fibrillation with adverse outcome.

Online supplemental material is available for this article.

[1] From the Laboratoire d'Imagerie Biomédicale, Sorbonne Universités, UPMC Univ Paris 06, INSERM 1146, CNRS 7371, 91 Boulevard de l'Hôpital, 75013 Paris, France (A.T.H., J.L., M.E., G.L., K.C., R.I., P.L., P.C., S.N.H., N.K., A.R.); Department of Cardiovascular and Thoracic Imaging and Interventional Radiology, Institute of Cardiology, Hôpital Pitié-Salpêtrière, Paris, France (A.T.H., P.C., N.K., A.R.); Institute of Cardiometabolism and Nutrition (ICAN), Paris, France (J.L., A.R., M.E., F.A., C.D., G.L., K.C., M.B., R.I., P.L., P.C., S.N.H., N.K., A.R.); INSERM UMR_1166, Paris, France (A.R., K.C., M.B., R.I., S.N.H.); Department of Cardiology, Institute of Cardiology, Hôpital Pitié-Salpêtrière, Paris, France (F.A., R.I., S.N.H.); and Department of Thoracic and Cardiovascular Surgery, Hôpital Pitié-Salpêtrière, Paris, France (C.D., G.L., P.L.). Received January 24, 2017; revision requested March 20; revision received May 4; accepted May 12; final version accepted May 24. **Address correspondence to** A.R. (e-mail: *alban.redheuil@aphp.fr*).

Supported by Institut Universitaire d'Ingénierie en Santé (ANR-10-IAHU-05), Institute of Cardiometabolism and Nutrition (ICAN research grant), Horizon 2020 Framework Programme, Schweizerische Akademie der Medizinischen Wissenschaften (Helmut-Hartweg-Foundation Research Grant HH-05/15), and Recherche Hospitalo-Universitaire en santé (ANR-15-RHUS-0003).

N.K. and A.R. contributed equally to this work.

Atrial fibrillation (AF) is the most frequent cardiac arrhythmia in clinical practice, and it is a major cause of stroke (1) and heart failure (2). Most often, AF is associated with profound structural and functional alterations of the atrial myocardium, promoting a true atrial cardiomyopathy. Fibrosis, which can be interstitial or packed with adipose deposits, particularly in the subepicardium (3), is an important component of atrial cardiomyopathy (4). This histologic remodeling and alterations in the excitation-contraction process of atrial myocytes contribute to the development of the arrhythmogenic substrate of AF.

Atrial cardiomyopathy can precede arrhythmia and is favored by heart failure, valve diseases, hypertension, obesity, and aging (5,6). Furthermore, its severity is an important determinant of AF recurrence (7,8) and response to treatment (9,10). In this context, it is of major clinical interest to have a noninvasive biomarker with which to quantify the degree of atrial cardiomyopathy. New imaging biomarkers could lead to early clinical decisions prior to new-onset AF or in patients with moderate mitral regurgitation, thus preventing the development of heart failure.

Several studies have investigated imaging methods to assess left atrial (LA) cardiomyopathy, such as ventricular and atrial late-gadolinium-enhancement (LGE) (11,12) T1 mapping (13). Others assessed LA wall strain with echocardiographic speckle tracking (14) or magnetic resonance (MR) imaging feature tracking (15). The concepts of these methods are different, since T1 mapping and LGE are used to directly investigate structural properties of the LA myocardium, while strain measurement is based on LA wall elastic function and mechanics. An association between LA strain and LA LGE has been reported (16). However, the maximum spatial resolution achieved in vivo with LGE sequences around 1 mm (17) is questionable to assess the 1–2-mm thick LA wall, as it is prone to partial volume effects (18). Precise strain measurement is more dependent on temporal resolution than on spatial resolution and is attainable with cardiac MR imaging cine steady-state free precession sequences (19).

LA echocardiographic speckle tracking was shown to enable prediction of cardiovascular outcomes (20), and it correlates with histologic interstitial fibrosis grade (21). The purpose of our study was to determine whether LA strain quantification with cardiac MR imaging feature tracking is associated with the severity of LA fibrofatty myocardial remodeling at histology.

Advances in Knowledge

- Decreased left atrial (LA) longitudinal strain measured with MR imaging in humans is strongly associated with increased fibrofatty myocardial replacement at histologic analysis ($r = -0.75$, $P = .017$).
- LA longitudinal strain is significantly lower in patients with mitral regurgitation than in healthy control subjects ($P < .001$), even in the absence of atrial fibrillation ($P = .003$).
- LA longitudinal strain measured with MR feature tracking is highly reproducible, with low interobserver coefficients of variation (5.4%) that are comparable to conventional left ventricular volumes (3.7%), for which MR imaging is an established reference modality.

Implications for Patient Care

- LA longitudinal strain may act as a noninvasive surrogate of LA fibrofatty remodeling and may ultimately be useful for early clinical decisions in patients prior to atrial fibrillation onset, a major and increasing cause of stroke and heart failure in aging populations.
- LA cardiomyopathy determined noninvasively using MR imaging strain may also influence early clinical treatment decisions in patients with mitral regurgitation.

Materials and Methods

Study Population

This prospective case-control study was approved by our institutional review board, and signed informed consent was given by all participants. All adult patients undergoing open surgery for mitral regurgitation without cardiocirculatory assist devices were eligible. Exclusion criteria were contraindications to cardiac MR imaging and inability to perform cardiac MR imaging in the 24 hours prior to cardiac surgery. Thirteen patients (nine male, four female) undergoing mitral valve replacement with left atriotomy in our cardiac surgery department were included consecutively between January 2014 and March 2015. Cardiac MR imaging was also performed in 13

https://doi.org/10.1148/radiol.2017162787

Content code: CA

Radiology 2018; 0:1–10

Abbreviations:
AF = atrial fibrillation
EDV = end-diastolic volume
EF = ejection fraction
ESV = end-systolic volume
LA = left atrium
LV = left ventricle
LGE = late gadolinium enhancement
PLAS = peak longitudinal atrial strain
PRAM = peak radial atrial motion fraction
ROC = receiver operating characteristic

Author contributions:
Guarantors of integrity of entire study, A.T.H., J.L., M.E., P.C., N.K., A.R.; study concepts/study design or data acquisition or data analysis/interpretation, all authors; manuscript drafting or manuscript revision for important intellectual content, all authors; approval of final version of submitted manuscript, all authors; agrees to ensure any questions related to the work are appropriately resolved, all authors; literature research, A.T.H., J.L., F.A., C.D., G.L., P.C., N.K.; clinical studies, A.T.H., J.L., M.E., C.D., G.L., R.I., P.L., P.C., N.K., A.R.; experimental studies, J.L., A.R., M.E., F.A., C.D., M.B.; statistical analysis, A.T.H., J.L., A.R., C.D., N.K., A.R.; and manuscript editing, A.T.H., J.L., C.D., K.C., R.I., P.L., P.C., S.N.H., N.K., A.R.

Conflicts of interest are listed at the end of this article.

Figure 1

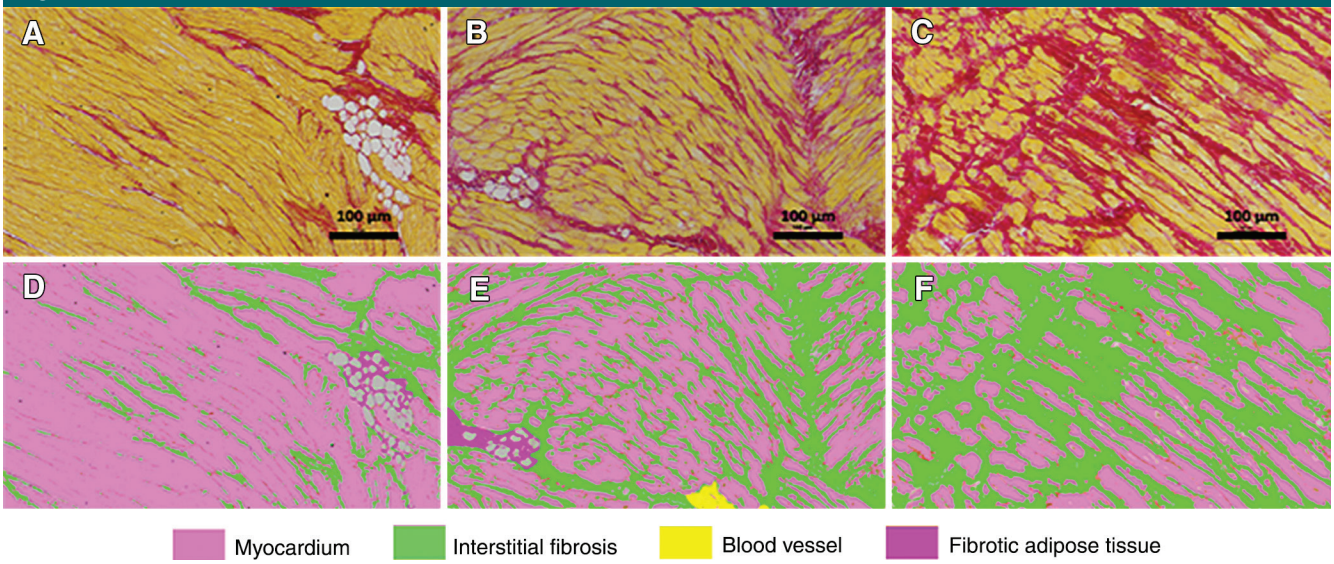

Figure 1: Histologic quantitative analysis of left atrial tissue samples. *A–C,* Representative photomicrographs of picrosirius red–stained atrial myocardial slices show various degrees of fibrosis in red, fat in white, and myocytes in yellow. Images were obtained, *A,* in a 32-year-old female patient with 27% fibrofatty myocardial replacement, *B,* in a 59-year-old male patient with 36% fibrofatty myocardial replacement, and, *C,* in a 35-year-old female patient with 58% fibrofatty myocardial replacement. *D–F,* Corresponding semiautomated histologic segmentation enables the exact quantification of myocytes, interstitial fibrosis, and intramyocardial fat.

age- and sex-matched healthy volunteers who were free of cardiovascular disease. These subjects comprised the control group. Thus, a total of 26 participants were included in this study. In three patients, LA biopsy material was insufficient to warrant state-of-the-art histologic analysis; therefore, histologic findings in correlation to cardiac MR imaging feature tracking were available in 10 patients. Three (23%) of 13 patients with new-onset mitral valve regurgitation detected in the 4 weeks prior to surgery were classified as having acute mitral regurgitation, while the remaining 10 (77%) patients were classified as having chronic mitral regurgitation. Five of 13 (38%) patients were in AF at the time of cardiac MR imaging (three permanent AF, two paroxysmal AF), while eight (62%) of 13 were in sinus rhythm.

Tissue Sample and Histologic Analysis

During open mitral valve replacement, a tissue sample was taken from the atriotomy border between the right pulmonary veins and the inferior vena cava on the LA inferomedial wall and fixed in neutral buffered paraformaldehyde 4%. The samples were then embedded in paraffin and stained with Picro-Sirius red for histologic analysis. Myocardial fibrosis, myocytes, and intramyocardial fat were semiautomatically segmented on the whole slides by using HistoLab, version 10.2.1 (Microvision Instruments, Evry, France) by a pathologist (F.A., 6 years of experience in cardiac histology) who was blinded to clinical information and strain results, allowing quantification of the different myocardial components (Figs 1, 2).

Cardiac MR Imaging Protocol

All subjects underwent a routine clinical protocol performed with a 1.5-T imager (Magnetom Aera; Siemens Healthcare, Erlangen, Germany) that included steady-state free precession short-axis views and longitudinal two-, three-, and four-chamber views covering the whole heart. The following MR imaging parameters were used: repetition time msec/echo time msec, 50.58/1.16; acquisition matrix, 232 × 256; flip angle, 59°; pixel size, 1.48 × 1.48 mm; section thickness, 6 mm; spacing between sections, 7 mm. Temporal resolution was 10–40 msec.

Assessment of Cardiac Volumes and Function

Left ventricular (LV) and right ventricular volumes and ejection fraction (EF) and LV mass were assessed by using Medis Suite 2.0.16.0 (Medis Medical Imaging Systems, Leiden, the Netherlands). LA systolic and diastolic volumes were estimated by using the biplanar area-length method (22). LA end-diastolic volume (EDV) was defined as the maximum volume in LA diastole, while LA end-systolic volume (ESV) was the minimal volume in LA systole. LA EF and mitral regurgitation volume were calculated from LA and LV volumes. Furthermore, patients underwent mitral regurgitation quantification with Doppler echocardiography prior to surgery, with use of the effective regurgitant orifice area, measured with the proximal isovelocity surface area method, as well as the *E*/*A* and *E*/*E'* ratios, with *E* being the early diastolic velocity peak; *A*, the late diastolic velocity peak in continuous transmitral Doppler, and *E'*, the early diastolic peak of lateral mitral annulus displacement velocity in tissue Doppler imaging.

Figure 2

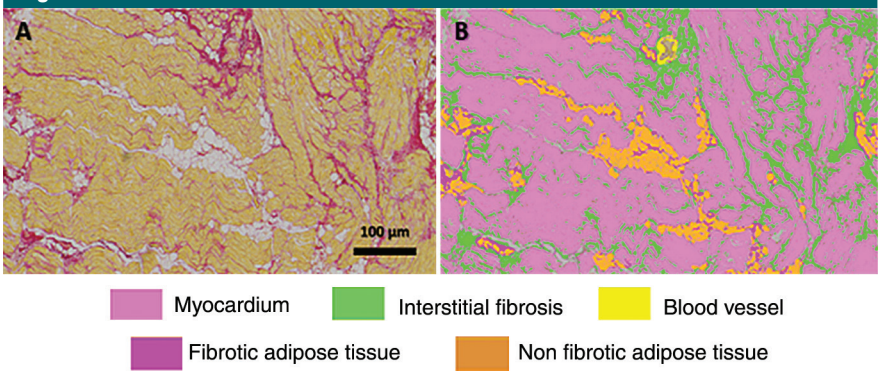

Figure 2: Histologic quantitative analysis of a sample with important fibrofatty myocardial replacement. *A,* Representative photomicrograph of a picrosirius red–stained atrial myocardial slice in a 64-year-old male patient shows fibrosis in red, fat in white, and myocytes in yellow. *B,* Corresponding semiautomated histology image shows total fibrofatty replacement of 38%.

Feature Tracking

LA feature tracking was performed by using dedicated cardiac MR imaging feature-tracking software (24). The endocardial borders were manually traced by two independent blinded reviewers (J.L., A.H.; 3 and 6 years of experience in cardiac imaging, respectively) on a drag-and-draw basis on a single-phase steady-state free precession cine image corresponding to atrial diastole. To be equally distributed on all segments, markers were automatically defined as the crossings of radii originating from the LA center of mass and the endocardial border. Imaging features in a 6 × 6 pixel region of interest around these markers were used to track the endocardial border throughout the cardiac cycle by using spatial correlation. Finally, an elastic constraint was applied on resulting endocardial contours. Longitudinal strain was defined as the temporal variation of the LA contour length and was calculated as $(L_{(t)}-L_0)/L_0$, where L_0 is the initial length and $L_{(t)}$ is the length at a given time. The radial motion fraction was defined as the radial relative displacement toward the LA center of mass.

Global and per-segment longitudinal strain and radial motion fraction were assessed separately in two-, three-, and four-chamber views. Mean strain was calculated as the mean of the three global strains. The analyzed metrics were peak longitudinal atrial strain (PLAS) and peak radial atrial motion fraction (PRAM) corresponding to the atrial reservoir function, as well as pre a-wave longitudinal strain and radial atrial motion fraction corresponding to the LA booster pump function. Strain rates were calculated as the first temporal derivative of the strain curves: PLAS and PRAM rate was calculated as the first positive peak (reservoir function), E wave longitudinal strain rate and radial motion rate (E-S rate and E-M rate, respectively) was calculated as the first negative peak (atrial conduit function), and A wave longitudinal strain rate and radial motion rate (A-S rate and A-M rate, respectively) was calculated as the second negative peak (atrial booster pump function) (Fig 3). In addition to global LA strains, regional strain values were calculated in the anterior, posterior, inferior, lateral, and septal LA wall.

Reproducibility

Cardiac MR imaging LA volumetry, LV volumetry, and LA strain measurements were assessed by two independent readers (J.L., A.H.) to analyze the reproducibility.

Follow-up

All patients were contacted by telephone between 12 and 27 months (mean, 22 months) after mitral valve surgery to collect clinical follow-up information. Follow-up was achieved in nine of 13 patients, as four patients were lost to follow-up. At follow-up, the nine patients felt subjectively better than they felt before surgery, and all had a New York Heart Association score greater than or equal to III. All of the patients with AF before surgery still had paroxysmal or permanent AF, with the exception of one patient who underwent heart transplantation. None of the patients without preoperative history of AF had AF at follow-up.

Statistical Analyses

Our sample size was based on the findings of Kowallick et al (23), who showed that a sample size of seven patients per group is sufficient to detect a 10% difference and that a sample size of four is sufficient to detect a 15% difference of PLAS by using MR imaging feature tracking with a power of 90% and an α error of .05. This translates to our study sample size of 13 patients (five in AF, eight in sinus rhythm) and 13 control subjects. Statistical analysis was performed with Stata software (version 11.2; Stata, College Station, Tex) and GraphPad Prism (version 7.1; GraphPad Software, La Jolla, Calif). Comparisons between groups were performed by using the nonparametric Mann-Whitney test for continuous variables and the Fisher exact test for categorical variables. These analyses were performed in all patients and were compared with the control group, as well as between patients with acute and chronic mitral regurgitation and between patients in sinus rhythm and AF separately. Spearman correlation was used to study the association of the histologic LA myocardial fat and fibrosis composition with the measured LA global and regional strain and LA volume parameters. Receiver operating characteristic (ROC) analysis was used to obtain the optimal cutoff values of LA strain parameters and LA volumetry to differentiate between patients with mitral regurgitation and healthy control subjects. Leave-one-out cross-validation was used to calculate mean sensitivity and specificity of the ROC curves with

Figure 3

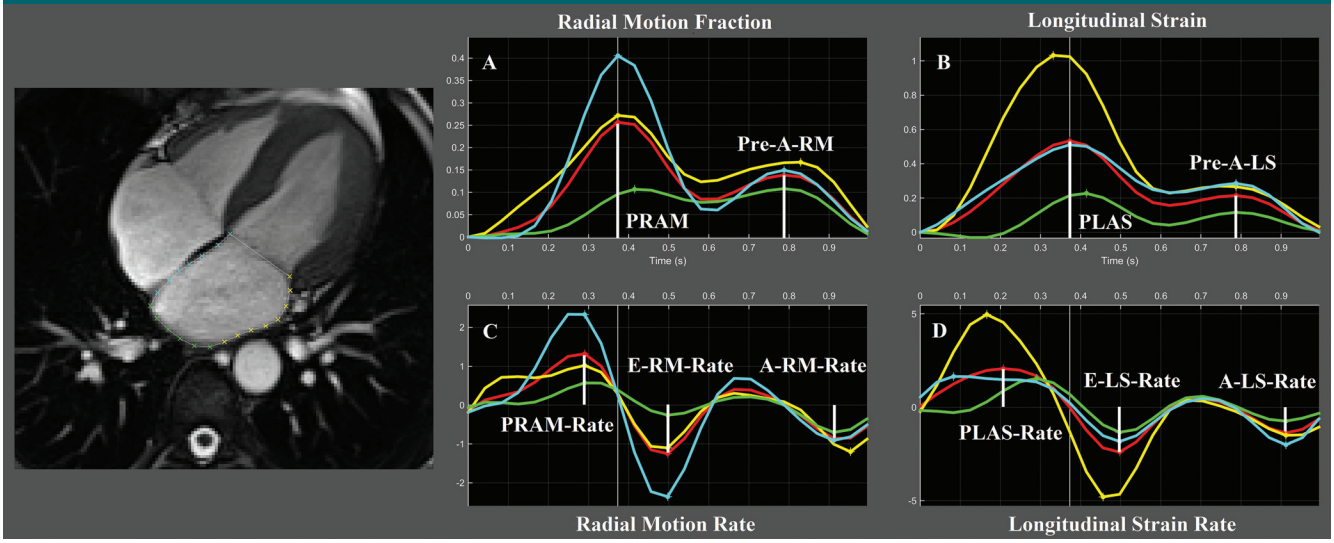

Figure 3: LA strain measurements on a four-chamber steady-state free precession cine view in a 63-year-old male healthy volunteer. *A,* PRAM and, *B,* PLAS correspond to LA reservoir function, while pre-A-wave longitudinal strain *(pre-A-LS)* and pre-A-wave radial motion fraction *(pre-A-RM)* correspond to atrial booster pump function. *C, D,* Strain rate peaks correspond to the longitudinal and radial reservoir (PRAM rate in *C,* PLAS rate in *D*), conduit (E-M rate in *C*, E-S rate in *D*), and booster pump (A-M rate in *C,* A-S rate in *D*) function. Red = global strain and strain rates, yellow, green, and blue correspond to LA segmental measurements on the cardiac MR image (left).

standard deviations. Cutoff values were identified on the averaged ROC curve by using the Youden index. Coefficients of variation were calculated between two independent readers for LA volumetry, LV volumetry, and LA strain parameters to assess interrater variability. $P < .05$ indicated a significant difference.

Results

The baseline characteristics of the study population are listed in Table 1. The patients in sinus rhythm and the patients in AF matched the age of the healthy control subjects. Patients in AF took more antihypertensive drugs than did patients in sinus rhythm. On the other hand, they showed less mitral valve prolapse associated with dystrophy; however, they tended to have more rheumatic, infectious, and ischemic causes of mitral valve disease. Mitral regurgitation quantification with Doppler echocardiography showed no significant differences in the effective regurgitant orifice area between patients in sinus rhythm (mean, 0.77 cm^2 ± 0.33 [standard devitation]) and those in AF (mean, 0.60 cm^2 ± 0.41; $P = .51$). Moreover, no significant differences were found between the two groups in terms of diastolic function indexes (E/A ratio, $P = .99$; E/E' ratio, $P = .51$).

All LA strains and strain rates were significantly different between patients with mitral regurgitation and control subjects, with the exception of longitudinal E-S rate (Table 2). Patients with mitral regurgitation had lower strain values, higher LA volumes, and lower LA EF than did control subjects. The same held true for patients with AF as compared with patients in sinus rhythm. The performance of PLAS as the overall best strain parameter is shown in more detail in Figure 4. Cardiac MR imaging parameters, including LV and LA volumetry and mean strain values, are presented in Table 2.

To assess interrater variability, coefficients of variation between two independent readers were calculated as follows: LV EDV, 3.7%; LV ESV, 7.2%; LV EF, 3.6%; LA EDV, 6.5%; LA ESV, 8.0%; LA EF, 22.6%; PLAS, 5.4%; pre-A-wave longitudinal strain, 15.7%; PLAS rate, 9.3%; longitudinal, E-S rate, 8.7%; and longitudinal A-S rate, 19.9%. Interrater variability of PLAS was thus comparable to the standard measurements of LV EDV, LV ESV, and LV EF.

Best correlation was achieved between a decrease in global PLAS and an increase in total fat and fibrosis in the myocardium ($r = -0.75$, $P = .017$). In addition to global LA strains, regional PLAS correlated well with histology when estimated at the anatomic location where the tissue sample was taken ($r = -0.78$, $P = .011$) and when estimated for the lateral free wall ($r = -0.83$, $P = .005$). This correlation was lower for PLAS of less mobile LA segments between the pulmonary veins ($r = -0.65$, $P = .049$) and the interatrial septal wall ($r = -0.48$, $P = .166$). Patients with chronic mitral regurgitation showed significantly lower strain values and higher degree of myocardial fibrofatty replacement than did patients with acute mitral regurgitation. Of note, all of the patients with acute mitral regurgitation had a moderate degree of histologic LA fibrofatty replacement and intermediate LA strain values. There was no significant correlation between any strain value and myocardial fat alone. Detailed correlation coefficients between different LA strain parameters

Table 1

Baseline Characteristics of the Study Population

Characteristic	Control Subjects ($n = 13$)	Patients ($n = 13$)	*P* Value	Patients in Sinus Rhythm ($n = 8$)	Patients in AF ($n = 5$)	*P* Value
Age (y)*	57 ± 9	61 ± 19	.426	62 ± 20	59 ± 20	.942
Sex (M/F)	9/4	9/4	>.999	2 (25%)	2 (40)	>.999
Body mass index (kg/m^2)*	25 ± 5	24 ± 3	.739	24 ± 3	25 ± 4	.435
New York Heart Association functional classification ≥III	0 (0)	7 (55)	.005	3 (38)	4 (80)	.266
Chronic renal failure	0 (0)	3 (23)	.220	1 (13)	2 (40)	.511
One or more cardiovascular risk factor	0 (0)	5 (38)	.039	3 (38)	2 (40)	>.999
NT-proBNP level (pg/mL)	…	4404 ± 5818	…	3987 ± 6001	4989 ± 6191	.268
Antihypertensive drugs						
≥1	0 (0)	12 (92)	<.001	7 (88)	5 (100)	>.999
≥2	0 (0)	7 (55)	.005	2 (25)	5 (100)	.021
Atrioventricular blockage	0 (0)	2 (15)	.480	2 (25)	0 (0)	.487
Mitral valve prolapse	0 (0)	9 (69)	<.001	7 (88)	2 (40)	.217
Mechanism						
Dystrophy	0 (0)	9 (69)	<.001	7 (88)	2 (40)	.217
Rheumatic	0 (0)	2 (15)	.480	1 (13)	2 (40)	.511
Endocarditis	0 (0)	2 (15)	.480	1 (13)	1 (20)	>.999
Ischemic	0 (0)	1 (8)	>.999	0 (0)	1 (20)	.385
Treatment						
Annuloplasty	0 (0)	9 (69)	<.001	7 (88)	2 (40)	.217
Valve replacement	0 (0)	3 (23)	.220	1 (13)	2 (40)	.511
Transplantation	0 (0)	1 (8)	>.999	0 (0)	1 (20)	.417

Note.—Unless otherwise indicated, data are number of patients, and data in parentheses are percentage. *P* values were calculated with the Mann-Whitney *U* test or Fisher exact test, as appropriate. NT-proBNP = *N*-terminal pro–B-type natriuretic peptide.

* Data are mean ± standard deviation

and histologic findings are shown in Table E1 (online).

Even if PLAS and LA EF were strongly linked (Fig 5), there was no significant correlation between LA myocardial fibrofatty replacement and LA volumes ($r = 0.18$, $P = .632$ for LA EDV; $r = -0.38$, $P = .279$ for LA EF). However, ROC analysis with leave-one-out cross-validation revealed that LA EDV was a good index with which to differentiate patients with mitral regurgitation from healthy control subjects, with a mean area under the curve of 0.98 ± 0.01 ($P < .001$), a mean sensitivity of 86% ± 2, and a mean specificity of 100% ± 0 using a mean indexed LA EDV cutoff of more than 64 mL/m^2 ± 0.2. PLAS showed a slightly lower mean area under the curve of 0.92 ± 0.01 ($P < .001$) to differentiate patients with mitral regurgitation from control subjects. With an optimum mean PLAS cutoff value of less than 30% ± 1, differentiation between the two groups was possible with a mean sensitivity of 93% ± 8 and a mean specificity of 77% ± 3. A mean PLAS cutoff value of less than 12% ± 0.5 enables differentiation of patients with LA fibrofatty replacement at histology of more than 45% versus those with LA fibrofatty replacement at histology of less than 45%, with a mean sensitivity of 100% ± 0 and a mean specificity of 83% ± 6.

Discussion

Our results show that decreased LA strain, notably PLAS, is directly correlated to the histologic degree of LA fibrofatty remodeling, which is the morphologic substrate of LA cardiomyopathy. The two existing studies comparing echocardiographic speckle tracking and histologic findings reported a correlation between PLAS and fibrosis of −0.82 (21) and −0.55 (24). The correlation between PLAS and LA interstitial fibrosis in the present cardiac MR imaging study ($r = -0.66$ for fibrosis, $r = -0.75$ for fat and fibrosis) was consistent with such echocardiographic findings, although a direct comparison is rendered difficult by the differences in the studied populations. Indeed, Cameli et al (21) considered a more homogeneous patient population, excluding those with AF, diabetes, or hypertension. Our results also show a strong correlation between regional PLAS and myocardial fibrofatty infiltration in the LA segment, including at the atriotomy site where the tissue sample was taken ($r = -0.78$, $P = .01$). However, there was a slightly higher correlation with PLAS measured on the mobile lateral wall, while correlations were lower in less mobile LA segments (posterior segment between the pulmonary veins and septal wall). Our study population was too small to determine the extent to which these differences were due to heterogeneous fibrofatty remodeling of the LA wall due to regional variations

Table 2

MR Imaging Parameters

Parameter	Control Subjects ($n = 13$)	Patients ($n = 13$)	*P* Value	Patients in Sinus Rhythm ($n = 8$)	Patients in AF ($n = 5$)	*P* Value
LV						
EDV index (mL/m^2)	81 ± 14	117 ± 24	<.001	120 ± 24	113 ± 24	.622
ESV index (mL/m^2)	29 ± 6	58 ± 26	<.001	51 ± 16	69 ± 34	.354
Mass index (mL/m^2)	56 ± 14	69 ± 10	.010	70 ± 12	68 ± 9	.833
EF (%)	63 ± 7	51 ± 16	.030	57 ± 12	41 ± 18	.127
Mitral regurgitation fraction	…	43 ± 16	…	48 ± 19	36 ± 9	.435
LA						
EDV index (mL/m^2)	43 ± 14	92 ± 25	<.001	82 ± 20	107 ± 27	.127
ESV index (mL/m^2)	19 ± 7	65 ± 30	<.001	50 ± 21	89 ± 28	.019
EF (%)	56 ± 7	31 ± 17	<.001	39 ± 16	18 ± 6	.011
Mean longitudinal LA strain						
PLAS (%)	35.6 ± 8.6	17.0 ± 9.7	<.001	22.3 ± 8.6	8.5 ± 2.7	.011
Pre-A-LS (%)	17.7 ± 4.4	5.1 ± 4.8	<.001	6.8 ± 5.6	2.3 ± 0.6	.354
Mean longitudinal LA strain rate						
PLAS rate (%/sec)	1.43 ± 0.32	0.78 ± 0.37	<.001	0.97 ± 0.35	0.47 ± 0.12	.030
Longitudinal E-S rate (%/sec)	−1.34 ± 0.42	−0.92 ± 0.52	.026	−1.20 ± 0.47	−0.47 ± 0.14	.003
Longitudinal A-S rate (%/sec)	−1.42 ± 0.38	−0.50 ± 0.41	<.001	−0.68 ± 0.45	−0.23 ± 0.07	.093
Mean radial LA motion fraction						
PRAM (%)	24.2 ± 5.5	7.2 ± 5.5	<.001	10.1 ± 5.4	2.8 ± 0.6	.006
Pre-A-RM (%)	8.1 ± 2.8	2.8 ± 3.7	.001	4.0 ± 4.0	3.4 ± 8.7	.127
Mean radial LA motion rate						
PRAM rate (%/sec)	0.99 ± 0.26	0.41 ± 0.28	<.001	0.56 ± 0.26	0.18 ± 0.06	.006
Radial E-M rate (%/sec)	−0.82 ± 0.26	−0.51 ± 0.35	.014	−0.68 ± 0.35	−0.24 ± 0.11	.011
Radial A-M rate (%/sec)	−1.30 ± 0.39	−0.30 ± 0.29	<.001	−0.41 ± 0.31	−0.08 ± 0.08	.065

Note.—Data are mean ± standard deviation. *P* values were calculated with the Mann-Whitney *U* test. Longitudinal A-S rate/radial A-M rate = booster function longitudinal strain rate/radial motion fraction rate, longitudinal E-S rate/radial E-M rate = conduit function longitudinal strain rate/radial motion fraction-rate, pre-A-LS = pre-A-wave longitudinal strain, pre-A-RM = pre-A-wave radial motion fraction.

Figure 4

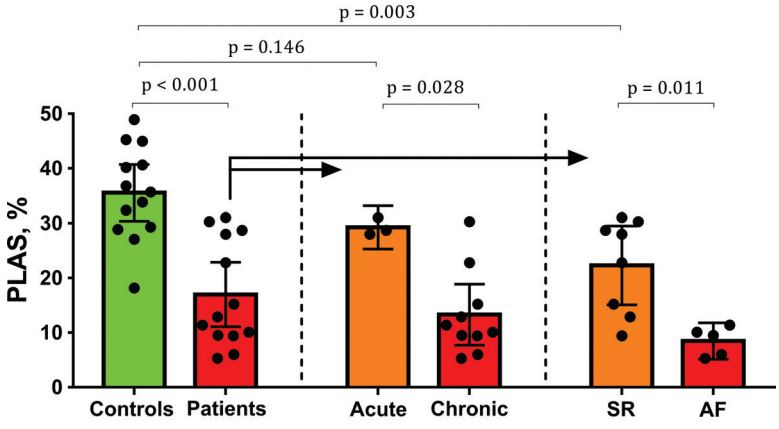

Figure 4: Graph shows PLAS in control subjects and patients with mitral regurgitation, as well as in patient subgroups. Comparison between the control group (mean age, 57 years ± 9, nine male) and all patients (mean age, 61 years ± 19, nine male) with mitral regurgitation is shown to the left of the first dashed line. Patients with mitral regurgitation are divided into those with acute (<4 weeks) mitral regurgitation and those with chronic (>4 weeks) mitral regurgitation, shown to the right of the first dashed line. Differentiation of patients in sinus rhythm and those in AF is shown on the side of the second dashed line.

of mechanical properties based on LA geometry.

Our results are also consistent with those in publications without histology. Ring et al (25) showed reduced LA reservoir and booster pump strain at echocardiography in patients with severe mitral regurgitation referred to surgery as compared with those without a surgical indication. In the present study, patients with chronic mitral regurgitation had significantly lower PLAS than did patients with acute mitral regurgitation. Moreover, PLAS was significantly lower in patients in AF when compared with PLAS in patients with mitral regurgitation in sinus rhythm. This is consistent with findings of recent cardiac MR imaging feature-tracking studies that show lower strain values in patients with AF when compared with those in healthy volunteers (16). The link between decreased PLAS and paroxysmal

Figure 5

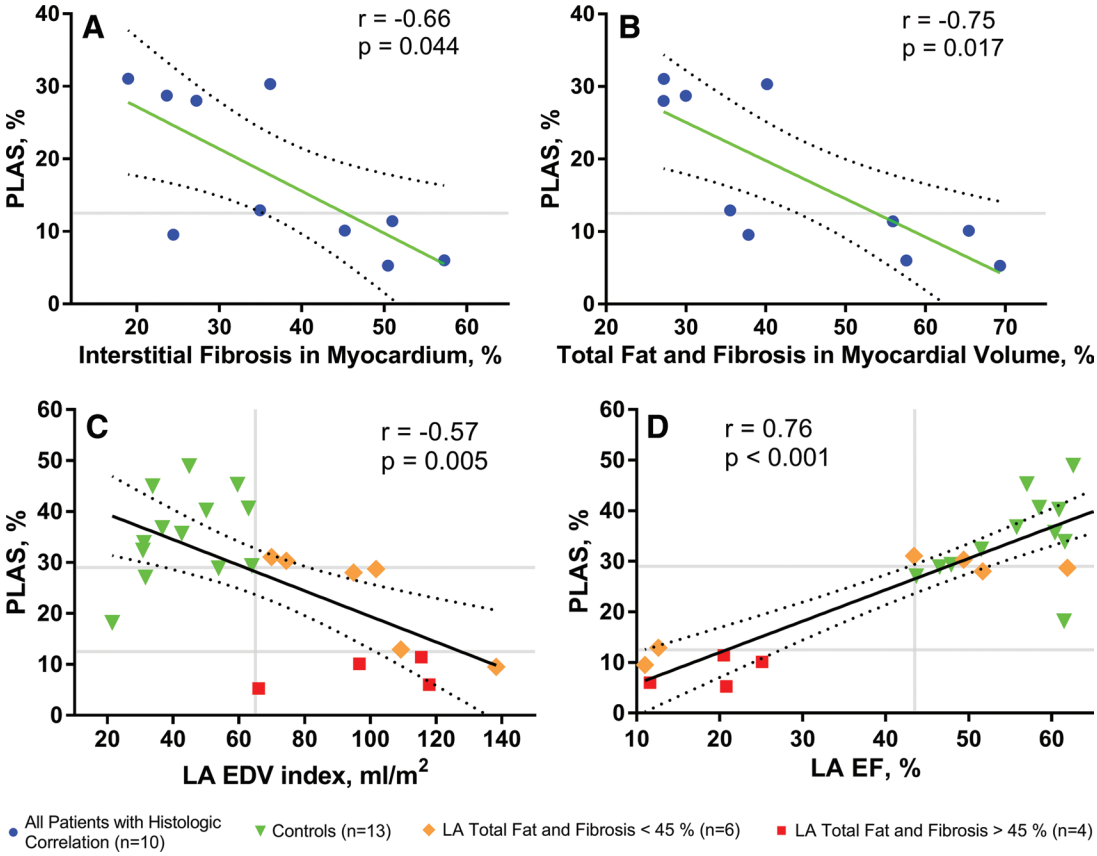

Figure 5: Graphs show Spearman correlation between PLAS, LA volumetry, and histology. On the first line, correlation between PLAS and histologic degree of myocardial remodeling is shown in, *A*, with myocardial interstitial fibrosis and in, *B*, with the total amount of fat and fibrosis in myocardial volume. *C, D,* Spearman correlation between PLAS and LA EDV in *C* and LA EF in *D*. Dashed lines indicate upper and lower 95% confidence intervals. Gray lines indicate cutoff values calculated with ROC analysis (65 mL/m^2 for LA EDV, 29% PLAS to differentiate between control subjects and patients and 12.5% PLAS to differentiate between patients with more or less than 45% of LA fibrofatty replacement).

AF in patients with mitral regurgitation is also consistent with the findings of echocardiographic speckle tracking studies (26). Of note, in our study, PLAS remained significantly lower in patients with mitral regurgitation, even in the absence of AF.

While significantly correlated with LA EF, PLAS and other strain indexes were stronger correlates of the histologic fibrofatty replacement grade, and LA EDV did not correlate with histologic findings. Nevertheless, LA EDV seemed to be useful to differentiate between patients with mitral regurgitation and healthy control subjects when using an LA EDV index cutoff of more than 65 mL/m^2. This cutoff is consistent with published normal indexed values of LA EDV (range, 26–52 mL/m^2) in healthy men (27,28) and with Kawel-Boehm et al (27) and Le Tourneau et al (28) showing that an LA EDV index greater than 60 mL/m^2 is associated with reduced 5-year survival. Consequently, LA EDV could be used to screen for possible LA involvement in patients with mitral regurgitation (LA EDV >65 mL/m^2). LA cardiomyopathy severity could then be graded by using LA strain in the selected patients. However, these observations will have to be confirmed in a larger population, especially in patients with causes of LA cardiomyopathy other than mitral regurgitation, since the increased LA EDV in this study could be a consequence of LA volume overload due to mitral regurgitation.

With the demonstration of a strong correlation between LA strain and degree of fibrofatty myocardial infiltration, LA strain and, notably, PLAS could be used as surrogate quantitative biomarkers for myocardial fibrofatty replacement in LA cardiomyopathy. Moreover, patients with acute mitral regurgitation and some patients with chronic mitral regurgitation had only moderate LA strain reduction and a moderate degree of LA fibrofatty replacement. On the other hand, all patients in permanent AF had severely reduced LA strain and marked LA fibrofatty replacement. Accordingly, one

might suggest that patients with moderately reduced LA strain would be prone to benefit from an earlier and more aggressive treatment to prevent them entering the vicious circle of LA cardiomyopathy and AF. These observations are consistent with the findings of Debonnaire et al (29) showing a worse outcome 6 years after mitral valve surgery in patients with preoperative PLAS less than 25% when using echocardiography speckle tracking. These findings are also in agreement with Multi-Ethnic Study of Atherosclerosis findings showing that augmented cardiac MR imaging LA volume indexes and reduced PLAS precede heart failure (2).

Interrater reproducibility was very good for PLAS; in fact, it was almost as good as interrater reproducibility of LV EDV and LV EF based on comparison of coefficients of variations between two independent readers in the same patient population. Indeed, the feature-tracking software used in this study is based on a fully automated algorithm after manual initialization on one image. Consequently, main sources of error are the initial endocardial contour and the peak detection on strain and strain rate curves. Since the A-wave peak can be difficult to identify in patients with mitral regurgitation and is absent in patients with AF, it is not surprising that the pre-A-wave longitudinal strain shows reproducibility that is inferior to that of PLAS.

The first limitation of this study was the relatively small study population. This reflects how difficult it is to obtain cardiac MR images in the 24 hours before mitral valve surgery and to obtain sufficient tissue samples in patients. However, the MR feature-tracking strain values showed significant differences across groups and correlated significantly with fibrosis and fibrofatty infiltration at histology. This is also consistent with findings of a recent study, which showed that populations of seven and four patients are sufficient to detect 10% and 15% differences in LA PLAS with a power of 90% and an α error of .05 (23), which translates to our patient population and subgroups with or without AF. Another limitation was the inherent restriction to a patient population with mitral regurgitation undergoing surgery with LA atriotomy. Nevertheless, this setting allowed for in vivo tissue sampling for histologic analysis, which would not have been possible in patients with new-onset AF or with LV diastolic dysfunction alone. These promising results should lead to studies in other patients with other causes of LA cardiomyopathy.

Cardiac MR imaging LA strain indexes and, notably, PLAS are strongly related to the degree of myocardial fibrofatty remodeling in LA cardiomyopathy and are highly reproducible. LA EDV was used to differentiate between patients with mitral regurgitation and healthy volunteers but did not correlate with the degree of LA myocardial tissue remodeling. A possible implication to guide clinical decisions in patients with mitral regurgitation or primary AF is that prevention is promising but remains to be proven in large clinical studies.

Disclosures of Conflicts of Interest: A.T.H. disclosed no relevant relationships. **J.L.** disclosed no relevant relationships. **A.R.** disclosed no relevant relationships. **M.E.** disclosed no relevant relationships. **F.A.** disclosed no relevant relationships. **C.D.** disclosed no relevant relationships. **G.L.** disclosed no relevant relationships. **K.C.** disclosed no relevant relationships. **M.B.** disclosed no relevant relationships. **R.I.** Activities related to the present article: disclosed no relevant relationships. Activities not related to the present article: received grants from Novartis and Servier; received personal fees from Novartis, Servier, Bayer, BMS, Zoll, Amgen, and Sanofi. Other relationships: disclosed no relevant relationships. **P.L.** disclosed no relevant relationships. **P.C.** disclosed no relevant relationships. **S.N.H.** disclosed no relevant relationships. **N.K.** disclosed no relevant relationships. **A.R.** disclosed no relevant relationships.

References

1. Hoit BD. Left atrial size and function: role in prognosis. J Am Coll Cardiol 2014;63(6):493–505.
2. Habibi M, Chahal H, Opdahl A, et al. Association of CMR-measured LA function with heart failure development: results from the MESA study. JACC Cardiovasc Imaging 2014;7(6):570–579.
3. Hatem SN, Redheuil A, Gandjbakhch E. Cardiac adipose tissue and atrial fibrillation: the perils of adiposity. Cardiovasc Res 2016;109(4):502–509.
4. Kottkamp H. Human atrial fibrillation substrate: towards a specific fibrotic atrial cardiomyopathy. Eur Heart J 2013;34(35):2731–2738.
5. Frustaci A, Chimenti C, Bellocci F, Morgante E, Russo MA, Maseri A. Histological substrate of atrial biopsies in patients with lone atrial fibrillation. Circulation 1997;96(4):1180–1184.
6. Ramadeen A, Laurent G, dos Santos CC, et al. n-3 Polyunsaturated fatty acids alter expression of fibrotic and hypertrophic genes in a dog model of atrial cardiomyopathy. Heart Rhythm 2010;7(4):520–528.
7. den Uijl DW, Delgado V, Bertini M, et al. Impact of left atrial fibrosis and left atrial size on the outcome of catheter ablation for atrial fibrillation. Heart 2011;97(22):1847–1851.
8. McGann C, Akoum N, Patel A, et al. Atrial fibrillation ablation outcome is predicted by left atrial remodeling on MRI. Circ Arrhythm Electrophysiol 2014;7(1):23–30.
9. Saxena A, Kapoor J, Dinh DT, Smith JA, Shardey GC, Newcomb AE. Preoperative atrial fibrillation is an independent predictor of worse early and late outcomes after isolated coronary artery bypass graft surgery. J Cardiol 2015;65(3):224–229.
10. Gillinov AM, Gelijns AC, Parides MK, et al. Surgical ablation of atrial fibrillation during mitral-valve surgery. N Engl J Med 2015;372(15):1399–1409.
11. Imai M, Ambale Venkatesh B, Samiei S, et al. Multi-ethnic study of atherosclerosis: association between left atrial function using tissue tracking from cine MR imaging and myocardial fibrosis. Radiology 2014;273(3):703–713.
12. Gal P, Marrouche NF. Magnetic resonance imaging of atrial fibrosis: redefining atrial fibrillation to a syndrome. Eur Heart J 2017;38(1):14–19.
13. Beinart R, Khurram IM, Liu S, et al. Cardiac magnetic resonance T1 mapping of left atrial myocardium. Heart Rhythm 2013;10(9):1325–1331.
14. Leung M, Abou R, Van Rosendael P, et al. Echocardiographic markers of left atrial fibrosis associated with the severity of atrial fibrillation. J Am Coll Cardiol 2016;67(13 Suppl):1809.
15. Evin M, Redheuil A, Soulat G, et al. Left atrial aging: a cardiac magnetic resonance feature tracking study. Am J Physiol Heart Circ Physiol 2016;310(5):H542–H549.
16. Habibi M, Lima JA, Khurram IM, et al. Association of left atrial function and left

atrial enhancement in patients with atrial fibrillation: cardiac magnetic resonance study. Circ Cardiovasc Imaging 2015;8(2): e002769.

17. Akcakaya M, Basha T, Tsao C, et al. High-resolution late gadolinium enhancement imaging with compressed sensing: a single-center clinical study [abstr]. J Cardiovasc Magn Reson 2016;18(Suppl 1):O56.
18. Appelbaum E, Manning WJ. Left atrial fibrosis by late gadolinium enhancement cardiovascular magnetic resonance predicts recurrence of atrial fibrillation after pulmonary vein isolation: do you see what I see? Circ Arrhythm Electrophysiol 2014;7(1): 2–4.
19. Evin M, Cluzel P, Lamy J, et al. Assessment of left atrial function by MRI myocardial feature tracking. J Magn Reson Imaging 2015;42(2):379–389.
20. Cameli M, Lisi M, Focardi M, et al. Left atrial deformation analysis by speckle tracking echocardiography for prediction of cardiovascular outcomes. Am J Cardiol 2012;110(2): 264–269.
21. Cameli M, Lisi M, Righini FM, et al. Usefulness of atrial deformation analysis to predict left atrial fibrosis and endocardial thickness in patients undergoing mitral valve operations for severe mitral regurgitation secondary to mitral valve prolapse. Am J Cardiol 2013;111(4):595–601.
22. Madueme PC, Mazur W, Hor KN, Germann JT, Jefferies JL, Taylor MD. Comparison of area-length method by echocardiography versus full-volume quantification by cardiac magnetic resonance imaging for the assessment of left atrial volumes in children, adolescents, and young adults. Pediatr Cardiol 2014;35(4):645–651.
23. Kowallick JT, Morton G, Lamata P, et al. Quantification of atrial dynamics using cardiovascular magnetic resonance: inter-study reproducibility. J Cardiovasc Magn Reson 2015;17:36.
24. Her AY, Choi EY, Shim CY, et al. Prediction of left atrial fibrosis with speckle tracking echocardiography in mitral valve disease: a comparative study with histopathology. Korean Circ J 2012;42(5):311–318.
25. Ring L, Rana BS, Wells FC, Kydd AC, Dutka DP. Atrial function as a guide to timing of intervention in mitral valve prolapse with mitral regurgitation. JACC Cardiovasc Imaging 2014;7(3):225–232.
26. Cameli M, Lisi M, Righini FM, Focardi M, Alfieri O, Mondillo S. Left atrial speckle tracking analysis in patients with mitral insufficiency and history of paroxysmal atrial fibrillation. Int J Cardiovasc Imaging 2012;28(7):1663–1670.
27. Kawel-Boehm N, Maceira A, Valsangiacomo-Buechel ER, et al. Normal values for cardiovascular magnetic resonance in adults and children. J Cardiovasc Magn Reson 2015;17:29.
28. Le Tourneau T, Messika-Zeitoun D, Russo A, et al. Impact of left atrial volume on clinical outcome in organic mitral regurgitation. J Am Coll Cardiol 2010;56(7): 570–578.
29. Debonnaire P, Leong DP, Witkowski TG, et al. Left atrial function by two-dimensional speckle-tracking echocardiography in patients with severe organic mitral regurgitation: association with guidelines-based surgical indication and postoperative (long-term) survival. J Am Soc Echocardiogr 2013;26(9): 1053–1062.